Journal of Thermal Engineering, Vol. 5, No. 5, pp. 482-497, October, 2019
Yildiz Technical University Press, Istanbul, Turkey

INVESTIGATION OF LORENTZ FORCE EFFECT ON STEADY NANOFLUID FLOW AND HEAT TRANSFER THROUGH PARALLEL PLATES

A. T. Akinshilo[1,*], A.O. Ilegbusi[2]

ABSTRACT

In this paper Lorentz force effect on steady fluid flow and heat transfer of nanofluid is examined. The nanofluid is transported through horizontal parallel plates with magnetic flux of uniform density acting perpendicular to the plates. The effects of thermo-fluidic parameters such as Schmidt number, viscosity and magnetic parameter on flow and heat transfer are presented. Other important heat and mass transfer parameters such as Nusselt and Sherwood numbers practically relevant were also studied. Obtained results from analytical solutions shows quantitative increase of Magnetic parameter varied within the range of 1-4 depicts increasing temperature distribution. Also results when compared with past literatures forms good agreement. Therefore study provides a good emphasis for the advancements of Nano fluidics such as micro mixing, friction reduction, energy conservation, and biological samples.

Keywords: *Steady Flow, Nanofluid, Horizontal Plates, Lorentz Force, Homotopy Perturbation Method*

INTRODUCTION

The transport of fluid through parallel surfaces has become increasingly high in most industrial and manufacturing applications today such as power transmission, polymer processing and heat exchangers. Owing to its efficient flow and heat transfer of fluids to its required destination. As energy pricing has become a significant factor in determining the mode of fluid transport, the need to manage heat transfer efficiently as led to renewed effort by scientist and engineers to research into more efficient ways of managing energy. In efforts to enhance heat transfer Abu Nada et al. [1] studied heat transfer under natural convection in horizontal concentric annuli using nanoparticles to increase heat transfer effect on the fluid flow. Heat transfer and flow over stretching sheet was investigated by Cortell [2] where study outcome reveals the influence of radiation on flow while Ellahi et al. [3] presented heat transfer of non-Newtonian fluid through two coaxial cylinders with porous media using variable viscosity, effect of heat transfer on nanoparticle under the influence of magnetism is analyzed. Mixed convection of nanofluid flow through square cavities where analyzed by Garoosi et al. [4-5] under two phase simulation without and with external heating where results show the effect of buoyancy on cavity flow. Shortly after Garoosi et al. [6] Investigated nanofluid flow in heat exchangers adopting the Buongiorno model of numerical technique, they discovered that at low Rayleigh number heat transfer decreases. Brownian motion and thermophoresis effects on slip flow of alumina/water were investigated by Malvandi and Ganji [7] where they showed effects of Nanoparticle concentration on heat transfer. Heat transfer over stretching surface was studied by Mehmood and Ali [8] presenting a three dimensional analytic solution employing the homotopy analysis method. Rashidi et al. [9] analyzed entropy generation in a rotating porous disk under steady flow condition considering the influence of magnetism with results revealing effect of entropy on temperature distribution. Rashidi et al. [10] in the bid to control wake and vortex shedding later considered heat transfer around a porous obstacle. Convective surface boundary condition was used by Shehzad et al. [11] to study three dimensional flow of Jeffery fluid presenting velocity and temperature distribution using series solutions obtained from non-linear equations. Later Shehzad et al. [12-13] investigated thermal radiative effects on mixed convection of thixotropic fluid, results reveal numerical values of wall shear and heat transfer rate. Flow and heat transfer in a rotating system was investigated by Sheikholeslami et al. [14] between stretching sheet and porous surface, discussing the effects of thermo-fluidics on flow and heat transfer. Two phase simulation of nanofluid was also investigated by Sheikholeslami et al. [15] using heat line model analyzing the effect of magnetism on heat and mass transfer.

This paper was recommended for publication in revised form by Regional Editor Jaap Hoffman Hoffman
[1]Mechanical Engineering Department; University of Lagos, Akoka-Yaba, Nigeria
[2]Mechanical Engineering Department; Yaba College of Technology, Yaba, Nigeria
**E-mail address: ta.akinshilo@gmail.com*
Orcid id: 0000-0002-6436-3420
Manuscript Received 25 December 2017, Accepted 11 January 2018

In recent years the need to improve the thermal conductivity of fluids as led to the addition of nanoparticles into base fluid, owing to the fact that nanoparticles have higher thermal conductivities, which enhances the overall energy transport during fluid flow. Therefore this creative approach has been widely adopted by researchers in the study of flow and heat transfer [16-39].Nanofluid displays characteristics of high heat transfer and enhanced flow character due to high thermal conductivity of nanoparticles which makes them potentially useful in medical, fuel cells and microelectronic processes.

Approximate analytical methods of solutions applied by researchers in study of the fluid flow include the pertubation method (PM),homotopy analysis method (HAM), homotopy pertubation method (HPM), adomian decomposition method (ADM) and Differential transformation method (DTM) [39-43] .Methods such as PM are limited owing to the problems of weak nonlinearities and artificial pertubation parameter which may be non existent in practical sense . The need to find an initial condition to satisfy the boundary condition makes methods such as DTM requires computational tools such as Matlab, Maple or Mathematica in handling a solution of large parameters resulting to large computational cost and time. Lack of rigorous theories for determining the initial approximation of the HAM , its auxilliary function and parameter restricts the HAM. Also the problem of finding the adomian polynomials makes the ADM not attractive to researchers. However the homotopy pertubation method been a relatively simplistic method of solving nonlinear, coupled equations due to its highly successive and accurate approximation making it a favourable analytical technique to researchers.

Motivated by past research works, the homtopy pertubation method (HPM) is used to investigate Lorentz force effect which is a resistive magnetic force type on steady nanofluid flow and heat transfer coneyed through horizontal parallel plates .

MODEL DEVELOPMENT AND ANALYTICAL SOLUTION

Here nanofluid flows through parallel plates held horizontally against each other under steady flow condition. The plates are held at a distance h, where the x axis is along the plate and the y axis is perpendicular which is described in the physical model of problem Figure 1. The nanofluid flow along the x axis which is normal to the plate with an angular velocity. A uniform magnetic flux acts perpendicular to the axis of flow, such that the plates is held by equal but opposite force which fixes its position at reference (0, 0, 0) i.e. its position remains the same. The formulation of the model development of the nanofluid is developed with respect to the above conditions following the assumptions that the fluid is incompressible, radiation heat transfer is negligible and two component mix is in thermal equilibrium. Therefore the governing equations of the system can be described as:

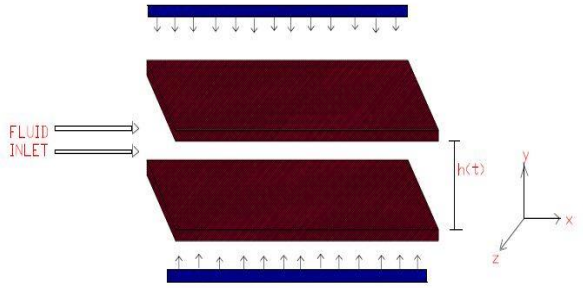

Figure 1. Physical model of problem

$$\frac{\partial u}{\partial x}+\frac{\partial v}{\partial y}=0 \tag{1}$$

$$\rho_f\left(u\frac{\partial u}{\partial x}+v\frac{\partial u}{\partial y}\right)=-\frac{\partial p^*}{\partial x}+\mu\left(\frac{\partial^2 u}{\partial x^2}+\frac{\partial^2 u}{\partial y^2}\right)-\sigma B_0^2 u \tag{2}$$

$$\rho_f\left(u\frac{\partial v}{\partial x}+v\frac{\partial T}{\partial y}\right)=-\frac{\partial p^*}{\partial y}+\mu\left(\frac{\partial^2 v}{\partial x^2}+\frac{\partial^2 v}{\partial y^2}\right) \tag{3}$$

$$u\frac{\partial T}{\partial x}+v\frac{\partial T}{\partial y}=\alpha\left(\frac{\partial^2 T}{\partial x^2}+\frac{\partial^2 T}{\partial y^2}\right)+\frac{(\rho Cp)_p}{(\rho Cp)_f}x\left[D_{\mathbf{B}}\left\{\frac{\partial C}{\partial x}\frac{\partial T}{\partial x}+\frac{\partial C}{\partial y}\frac{\partial T}{\partial y}\right\}+\left(D_T/\mathrm{T}_C\right)\left\{\left(\frac{\partial T}{\partial x}\right)^2+\left(\frac{\partial T}{\partial y}\right)^2\right\}\right] \tag{4}$$

$$u\frac{\partial C}{\partial x}+v\frac{\partial C}{\partial y}=D_B\left(\frac{\partial^2 C}{\partial x^2}+\frac{\partial^2 C}{\partial y^2}\right)+\left(\frac{D_T}{T_0}\right)\left\{\frac{\partial^2 T}{\partial x^2}+\frac{\partial^2 T}{\partial y^2}\right\} \tag{5}$$

Taking boundary conditions as:

$$u=ax, v=0, T=T_h, C=C_h \qquad \text{at y=0} \tag{6}$$

$$u=0, v=0, T=T_0, C=C_0 \qquad \text{at y=+h} \tag{7}$$

With the dimensionless parameters stated in the nomenclature, the dimensionless equations are given as [37]:

$$\frac{d^4 f}{\partial \eta^4}-R\left(\frac{df}{d\eta}\frac{d^2 f}{d\eta^2}+f\frac{d^2 f}{d\eta^2}\right)-M^2\frac{d^2 f}{d\eta^2}=0 \tag{8}$$

$$\frac{d^2\theta}{d\eta^2}+\mathrm{PrRf}\frac{d\theta}{d\eta}+Nb\frac{d\theta}{d\eta}\frac{d\phi}{d\eta}+Nt\left(\frac{d\theta}{d\eta}\right)^2=0 \tag{9}$$

$$\frac{d^2\phi}{d\eta^2}+RScf\frac{d\phi}{d\eta}+\frac{Nt}{Nb}\frac{d^2\theta}{d\eta^2}=0 \tag{10}$$

Taking appropriate boundary condition as:

$$f=0, \frac{df}{d\eta}=1, \theta=1, \phi=1 \text{ at } \eta=0 \tag{11a}$$

$$f=0, \frac{df}{d\eta}=0, \theta=0, \phi=0 \text{ at } \eta=1 \tag{11b}$$

Important characteristics of flow, heat and mass transfer for practical relevance are reduced to skin friction, Nusselt and reduced Sherwood number which can be defined as:

$$C_{fr} = f''(1) \text{ where } \mathrm{C}_{fr} = \frac{H^2\sqrt{1-\alpha t\,\mathrm{Re}_r}}{r^2} C_f \tag{12a}$$

$$Nur = -\theta'(1) \text{ where } Nur = \sqrt{1-\alpha t}Nu \tag{12b}$$

$$shr = -\phi'(1) \text{ where } \mathrm{shr} = \sqrt{1-\alpha t}sh \tag{12c}$$

where $\mathrm{Re}_r = \frac{r\alpha H}{2v}$ is the local squeeze Reynolds number.

Principles of Homotopy Perturbation Method

The following equation is considered in explaining the fundamentals of the homotopy perturbation method [38]:

$$A(u) - f(r) = 0 \quad r \in \Omega \tag{13}$$

Utilizing the boundary condition:

$$B(u, \frac{\partial u}{\partial \eta}) = 0 \quad r \in \Gamma \tag{14}$$

A is the general differential operator, B is the boundary operator, f(r) is the analytical function and Γ is the boundary domain of Ω. Separating A into two components of linear and nonlinear terms L and N respectively. The Eq. (13) is reconstructed as:

$$L(u) + N(u) - f(r) = 0 \quad r \in \Omega \tag{15}$$

Homotopy perturbation structure takes the form:

$$H(v, p) = (1-p)[\mathrm{L(v)} - \mathrm{L(u_0)}] + P[A(v) - f(r)] = 0 \tag{16}$$

where $v(r, p) : \Omega x[0,1] - R$

In Eq. (16) P ϵ (0, 1) is the embedding parameter and U_0 is taken as the initial term that satisfies boundary condition. The power series of Eq. (16) can be expressed therefore as:

$$v = v_0 + Pv_1 + P^2v_2 + P^3v_3 + ... \tag{17}$$

Most appropriate solution for the problem takes the form:

$$u = \lim_{p \to 1}(v_0 + Pv_1 + P^2 v_2 + P^3 v_3 + ...) \tag{18}$$

Application of the Homotopy Perturbation Method

The homptopy pertubation method (HPM) which is an analytical scheme for providing approximate solutions to the ordinary differential equations, is adopted in generating solutions to the coupled ordinary nonlinear differential equation .Upon constructing the homotopy, the Eqs. (8)- (10) can be expressed as:

$$H_1(\mathrm{p},\eta) = (1-p)\left[\frac{d^4 f}{\partial \eta^4}\right] + p\left[\frac{d^4 f}{\partial \eta^4} - R\left(\frac{df}{d\eta}\frac{d^2 f}{d\eta^2} + f\frac{d^2 f}{d\eta^2}\right) - M^2\frac{d^2 f}{d\eta^2}\right] \tag{19}$$

$$H_2(p,\eta) = (1-p)\left[\frac{d^2\theta}{d\eta^2}\right] + p\left[\frac{d^2\theta}{d\eta^2} + \mathrm{PrRf}\frac{d\theta}{d\eta} + Nb\frac{d\theta}{d\eta}\frac{d\phi}{d\eta} + Nt\left(\frac{d\theta}{d\eta}\right)^2\right] = 0 \tag{20}$$

$$H_3(p,\eta) = (1-p)\left[\frac{d^2\phi}{d\eta^2}\right] + p\left[\frac{d^2\phi}{d\eta^2} + RScf\frac{d\phi}{d\eta} + \frac{Nt}{Nb}\frac{d^2\theta}{d\eta^2}\right] = 0 \tag{21}$$

Taking the appropriate boundary condition as:

$$f = 0, \frac{df}{d\eta} = 1, \theta = 1, \phi = 1 \text{ at } \eta=0 \tag{22a}$$

$$f = 0, \frac{df}{d\eta} = 0, \theta = 0, \phi = 0 \text{ at } \eta=1 \tag{22b}$$

Taking power series of velocity, temperature and concentration fields yields:

$$f = P^0 f_0 + P^1 f_1 + P^2 f_2 + ... \tag{23}$$

$$\theta = P^0\theta_0 + P^1\theta_1 + P^2\theta_2 + ... \tag{24}$$

$$\phi = P^0\phi_0 + P^1\phi_1 + P^2\phi_2 + ... \tag{25}$$

Substituting Eq. (23) into (20) and selecting at the various order yields:

$$P^0 : \frac{d^4 f_0}{d\eta^4} \tag{26}$$

$$P^1 : \frac{d^4 f_1}{d\eta^4} - \frac{d^2 f_0}{d\eta^2} M + R \frac{d^2 f_0}{d\eta^2} f_0 - \frac{d^2 f_0}{d\eta^2} \frac{df_0}{d\eta} \tag{27}$$

$$P^2 : \frac{d^4 f_2}{d\eta^4} - \frac{d^2 f_1}{d\eta^2} M + R \frac{d^2 f_0}{d\eta^2} f_1 + \frac{d^2 f_1}{d\eta^2} f_0 - \frac{df_0}{d\eta} \frac{d^2 f_1}{d\eta^2} - \frac{df_1}{d\eta} \frac{d^2 f_0}{d\eta^2} \tag{28}$$

Substituting Eq. (24) into (21) and selecting at the various order yields:

$$P^0 : \frac{d^2 \theta_0}{d\eta^2} \tag{29}$$

$$P^1 : \frac{d^2 \theta_1}{d\eta^2} + N_t \left(\frac{d\theta_0}{d\eta} \right)^2 - N_b \frac{d\theta_0}{d\eta} \frac{d\phi_0}{d\eta} + \Pr R f_0 \frac{d\theta_0}{d\eta} \tag{30}$$

$$P^2 : \frac{d^2 \theta_2}{d\eta^2} + 2N_t \frac{d\theta_0}{d\eta} \frac{d\theta_1}{d\eta} + N_b \frac{d\theta_0}{d\eta} \frac{d\phi_1}{d\eta} + N_b \frac{d\theta_1}{d\eta} \frac{d\phi_0}{d\eta} + \Pr R \frac{d\theta_0}{d\eta} f_1 + \Pr R \frac{d\theta_1}{d\eta} f_0 \tag{31}$$

Substituting Eq. (25) into (22) and selecting at the various order yields:

$$P^0 : \frac{d^2 \phi_0}{d\eta^2} + \left(\frac{N_t}{N_b} \frac{d^2 \theta_0}{d\eta^2} \right) \tag{32}$$

$$P^1 : \frac{d^2 \phi_1}{d\eta^2} + \left(\frac{N_t}{N_b} \frac{d^2 \theta_1}{d\eta^2} \right) - RSc \frac{d\phi_0}{d\eta} f_0 \tag{33}$$

$$P^2 : \frac{d^2 \phi_2}{d\eta^2} + \frac{N_t}{N_b} \frac{d^2 \theta_2}{d\eta^2} + RSc \frac{d\phi_0}{d\eta} f_1 + RSc \frac{d\phi_1}{d\eta} f_0 \tag{34}$$

Taking leading order boundary condition as:

$$f_0 = 0, \frac{df_0}{d\eta} = 1, \theta_0 = 1, \phi_0 = 1 \text{ at } \eta=0 \tag{35a}$$

$$f_0 = 0, \frac{df_0}{d\eta} = 0, \theta_0 = 0, \phi_0 = 0 \text{ at } \eta=1 \tag{35b}$$

Simplifying Eq. (26) applying the boundary condition Eq. (35) yields:

$$f_0 = \eta^3 - 2\eta^2 + \eta \tag{36}$$

Simplifying Eq. (29) applying the boundary condition Eq. (35) yields:

$$\theta_0 = 1-\eta \tag{37}$$

Simplifying Eq. (32) applying the boundary condition Eq. (35) yields:

$$\phi_0 = 1-\eta \tag{38}$$

Taking the first order boundary condition as:

$$f_1 = 0, \frac{df_1}{d\eta} = 1, \theta_1 = 1, \phi_1 = 1 \text{ at } \eta=0 \tag{39a}$$

$$f_1 = 0, \frac{df_1}{d\eta} = 0, \theta_1 = 0, \phi_1 = 0 \text{ at } \eta=1 \tag{39b}$$

Simplifying Eq. (27) and applying the first order boundary condition Eq. (39) yields:

$$f_1 = \frac{17R\eta^7}{420} - \frac{5R\eta^6}{36} - \frac{R\eta^8}{280} - \eta^4\left(\frac{M}{6}+\frac{R}{6}\right) + \eta^5\left(\frac{M}{20}+\frac{13R}{60}\right) - \frac{\eta^2}{2}\left(\frac{2M}{15}+\frac{R}{84}\right) + \frac{\eta^3}{6}\left(\frac{11M}{10}+\frac{23R}{210}\right) \tag{40}$$

Simplifying Eq. (30) applying the first order boundary condition Eq. (39) yields:

$$\theta_1 = \frac{\Pr R\eta^5}{20} - \frac{\Pr R\eta^4}{6} + \frac{\Pr R\eta^3}{6} + \left(-\frac{N_b}{2}-\frac{N_t}{2}\right)\eta^2 + \left(\frac{N_b}{2}+\frac{N_t}{2}-\frac{\Pr R}{20}\right)\eta \tag{41}$$

Simplifying Eq. (33) applying the first order boundary condition Eq. (39) yields:

$$\begin{aligned}\phi_1 = {} & \left(\frac{RSc}{6} - \frac{N_t\, Pr\, R}{20N_b}\right)\eta^5 + \left(\frac{N_t\, Pr\, R}{6N_b} - \frac{RSc}{6}\right)\eta^4 + \left(\frac{RSc}{6} - \frac{N_t\, Pr\, R}{6N_b}\right)\eta^3 \\ & + \left(\frac{N_t}{2} + \frac{N_t^2}{2N_b}\right)\eta^2 + \left(\frac{N_t\, Pr\, R}{20N_b} - \frac{RSc}{20} - \frac{N_t}{2} - \frac{N_t^2}{2N_b}\right)\eta\end{aligned} \tag{42}$$

The coefficient p^2 for $f(\eta), \theta(\eta) and \phi(\eta)$ in Eqs. (28), (31) and (34) were too long to be mentioned here but it is expressed graphically in all the results and in the result validation, Table 1. Therefore substituting eq. (36) and (40) into the power series Eq. (23) yields:

$$\begin{aligned}f = {} & \eta^3 - 2\eta^2 + \eta + \frac{17R\eta^7}{420} - \frac{5R\eta^6}{36} - \frac{R\eta^8}{280} - \eta^4\left(\frac{M}{6}+\frac{R}{6}\right) \\ & + \eta^5\left(\frac{M}{20}+\frac{13R}{60}\right) - \frac{\eta^2}{2}\left(\frac{2M}{15}+\frac{R}{84}\right) + \frac{\eta^3}{6}\left(\frac{11M}{10}+\frac{23R}{210}\right) + \cdots\end{aligned} \tag{43}$$

Similarly substituting the Eqs. (37) and (41) into the power series Eq. (24) can be expressed as:

$$\theta = 1 - \eta + \frac{\Pr R\eta^5}{20} - \frac{\Pr R\eta^4}{6} + \frac{\Pr R\eta^3}{6} + \left(-\frac{N_b}{2} - \frac{N_t}{2}\right)\eta^2 + \left(\frac{N_b}{2} + \frac{N_t}{2} - \frac{\Pr R}{20}\right)\eta + \ldots \quad (44)$$

Also the Eqs. (38) and (42) upon substituting into the power series (25) is expressed as:

$$\phi = 1 - \eta + \left(\frac{RSc}{6} - \frac{N_t\, Pr\, R}{20N_b}\right)\eta^5 + \left(\frac{N_t\, Pr\, R}{6N_b} - \frac{RSc}{6}\right)\eta^4 + \left(\frac{RSc}{6} - \frac{N_t\, Pr\, R}{6N_b}\right)\eta^3 + \left(\frac{N_t}{2} + \frac{N_t^2}{2N_b}\right)\eta^2 + \left(\frac{N_t\, Pr\, R}{20N_b} - \frac{RSc}{20} - \frac{N_t}{2} - \frac{N_t^2}{2N_b}\right)\eta + \cdots \quad (45)$$

Table 1. Comparison of values for temperature and concentration when M=R=1, Ec=Pr=Sc=N_t=N_b=0.1, Pr=10

	θ(η)			ϕ(η)		
η	Sheikholeslami et al. [37]	Present work	Error %	Sheikholeslami et al. [37]	Present work	Error %
0	1.0000	1.0000	0.0000	1.0000	1.0000	0.0000
0.1	0.8562	0.8566	0.0004	0.9426	0.9429	0.0003
0.2	0.7209	0.7213	0.0004	0.8776	0.8779	0.0003
0.3	0.5590	0.5993	0.0003	0.7994	0.7996	0.0002
0.4	0.4912	0.4916	0.0004	0.7069	0.7072	0.0003
0.5	0.3954	0.3960	0.0004	0.6024	0.6027	0.0003
0.6	0.3094	0.3097	0.0003	0.4888	0.4891	0.0003
0.7	0.2293	0.2296	0.0003	0.3691	0.3695	0.0004
0.8	0.1524	0.1527	0.0003	0.2462	0.2467	0.0003
0.9	0.0763	0.0767	0.0004	0.1225	0.1229	0.0004
1.0	-0.000	-0.000	0.0000	-0.000	-0.000	0.0000

RESULTS AND DISCUSSION

The result obtained from the analytical solutions using the HPM is discussed in this section. As observed the validity of results when compared with solutions obtained in literature forms satisfactory agreement as depicted in Table 1.0. Effect of parameters on flow, heat transfer and concentration are reported graphically. With thermal fluidic parameters at various values on the velocity, temperature and concentration profile are presented. The Figure 2 shows the effect of viscosity parameter (R) on the velocity distribution, as depicted as R increases the velocity distribution increases slightly due to increase in fluid activation energy causing an increase in fluid motion with maximum effect near the lower plate. While it is shown from Figure 3 that velocity distribution decreases at increasing numerical values of Lorentz force or magnetic parameter (M) which can be physically explained by the decrease in momentum boundary layer thickness caused by magnetic force field whose effect is maximum towards the lower plate and falls rapidly towards the upper plate.

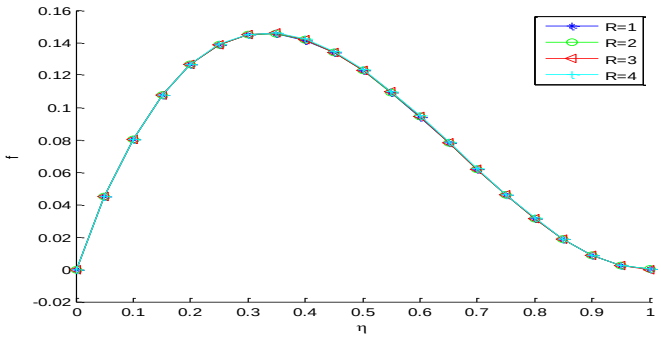

Figure 2. Effect of viscosity parameter (R) on velocity profile when Pr=10, Sc=N_t= N_b =0.1 and M=1

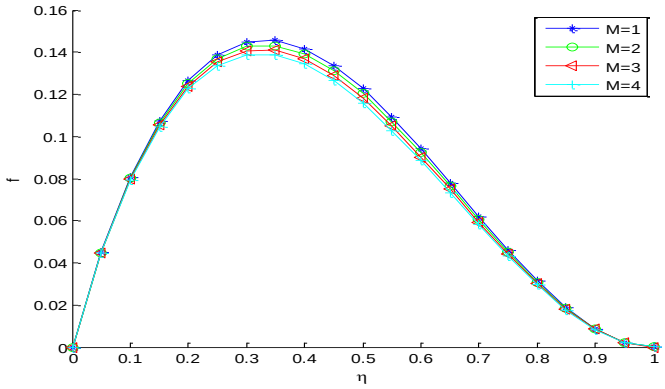

Figure 3. Effect of Magnetic parameter (M) on velocity profile when Pr=10,Sc=N_t= N_b =0.1 and R=1

The effect of increasing values of viscosity parameter (R) is demonstrated in Figure 4. It is observed that temperature distribution decreases at increasing R as a result of enhanced fluid motion causing rapid heat dissipation with the temperature profile maximum at the lower and minimum at the upper plate respectively. Magnetic parameter (M) effect on temperature distribution is clearly illustrated in Figure 5 which shows quantitative increase in M result in increasing thermal boundary layer thickness represented by slight increase in temperature. Increasing effect of thermophoretic parameter (N_t) on temperature distribution is seen in Figure 6 which depicts an increase in temperature profile while Brownian parameter (N_b) effect on temperature distribution is seen in Figure 7 where it is illustrated that increasing N_b gives a corresponding increase in temperature distribution.

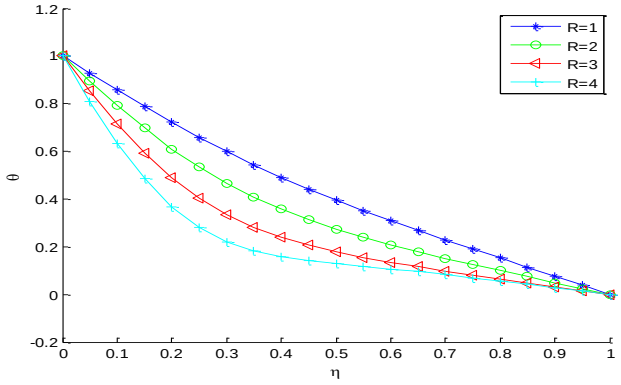

Figure 4. Effect of viscosity parameter (R) on Temperature profile when Pr=10,Sc=N_t= N_b =0.1 and M=1

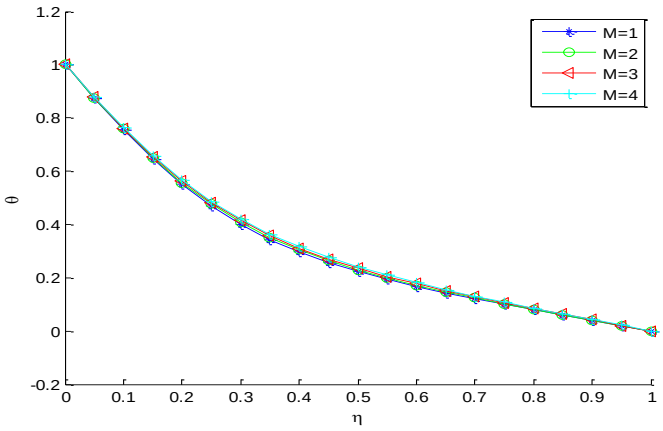

Figure 5. Effect of Magnetic parameter (M) on Temperature profile when Pr=10, Sc=N_t= N_b =0.1 and R=1

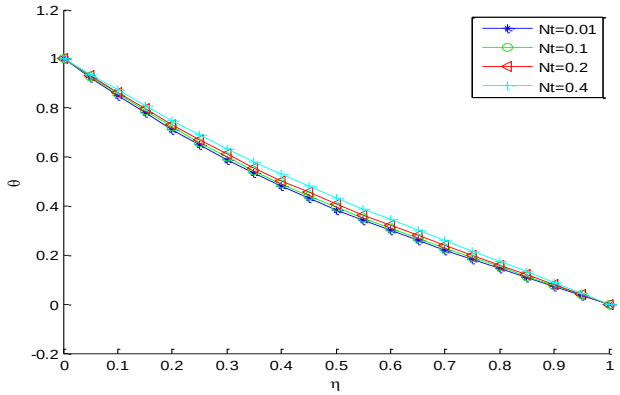

Figure 6. Effect of thermophoretic parameter (N_t) on Temperature profile when Pr=20, Sc= N_b =0.1 and M= R=1

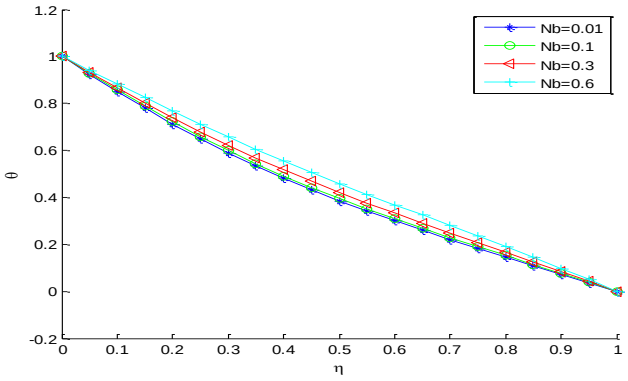

Figure 7. Effect of Brownian motion parameter (N_b) on Temperature profile when Pr=10, Sc= N_t =0.1 and M= R=1

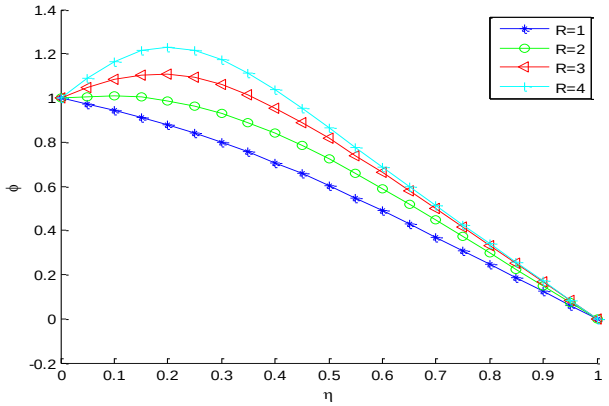

Figure 8. Effect of viscosity parameter (R) on concentration profile when Pr=10,Sc=N_t = N_b =0.1 and M=1

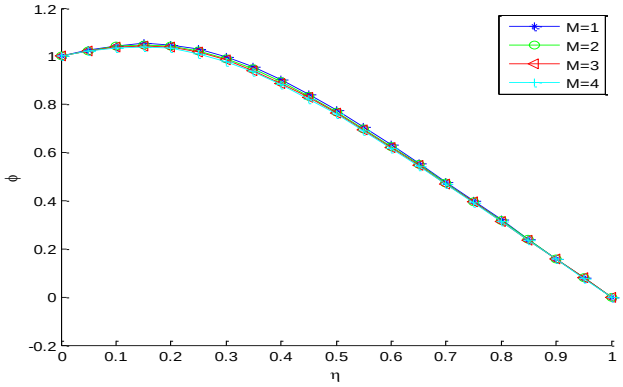

Figure 9. Effect of magnetic parameter (M) on concentration profile when Pr=10,Sc=N_t = N_b =0.1 and R=1

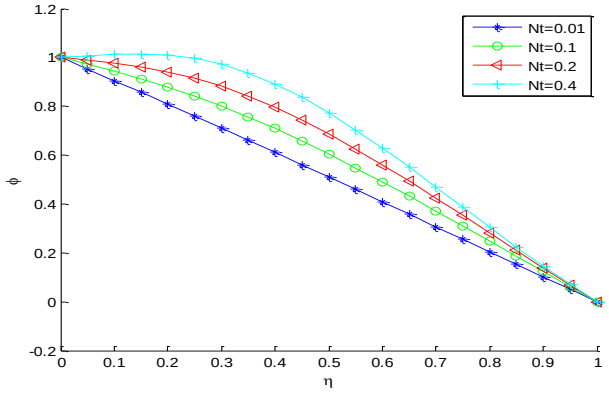

Figure 10. Effect of thermophoretic parameter (N_t) on concentration profile when Pr=10, Sc= N_b =0.1 and M= R=1

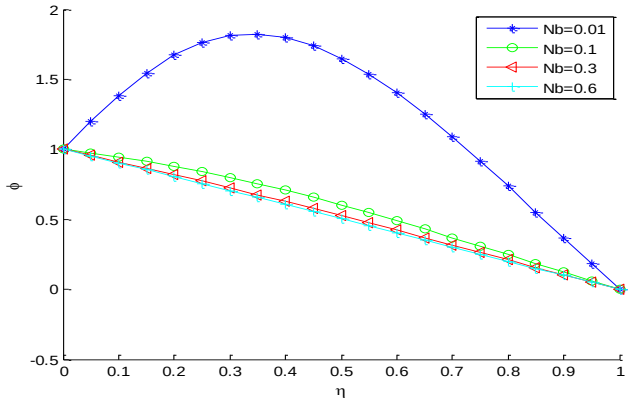

Figure 11. Effect of Brownian motion parameter (N_b) on concentration profile when Pr=10, Sc= N_t =0.1 and M= R=1

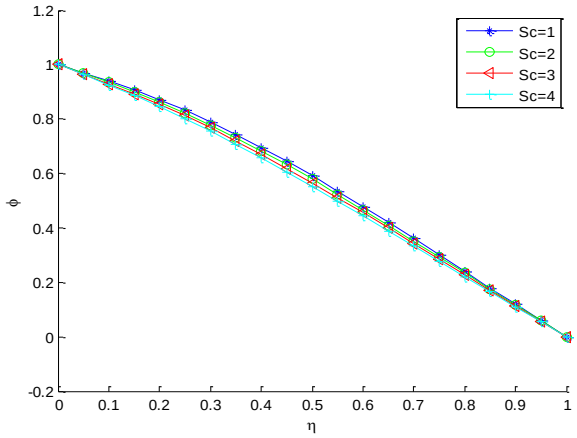

Figure 12. Effect of Schmidt number (Sc) on concentration profile when Pr=10, N_b= N_t =0.1 and M= R=1

Viscosity parameter (R) effect on Nano concentration is observed in Figure 8. It is shown that increasing R, concentration effect is maximum towards the lower plate due to increasing overall transport energy capacity. Magnetic parameter (M) effect on nanoparticle concentration is demonstrated in Figure 9 which depicts decreasing Nano concentration caused by increased magneto hydrodynamic boundary layer owing to higher thermal conductivity. It can be observed in Figure 10 that thermophoretic parameter (N_t) causes an increase in concentration profile as N_t increases quantitatively due to increasing fluid thermal diffusivity. Figure 11 depicts the effect of increasing values of Brownian motion parameter (N_b) on Nano concentration. As observed increasing values of N_b causes significant decrease in nano particle concentration owing to increased diffusion rate of reacting species. The effect of Schmit number (Sc) on concentration is observed in Figure 12. It is seen that increasing values of Sc leads to increased fluid viscosity causing a corresponding decrease in Nano concentration.

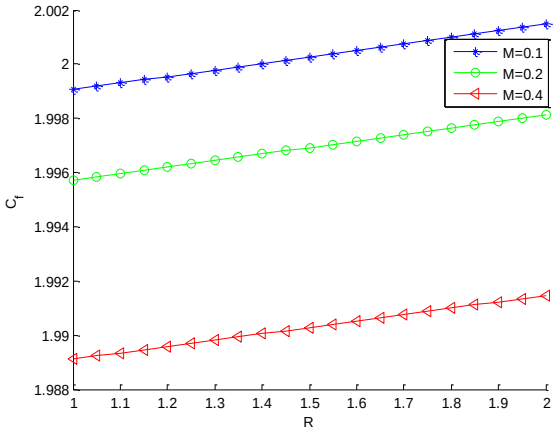

Figure 13. Effect of Magnetic parameter (M) on skin friction when Pr=10, N_b= N_t =0.1

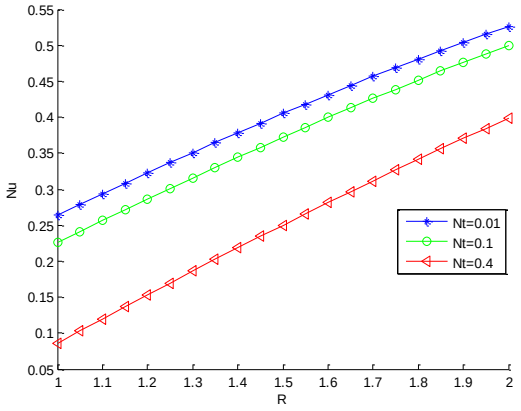

Figure 14. Effect of thermophoretic parameter (N_t) on Nusselt number when Pr=10, N_b =0.1 and M=1

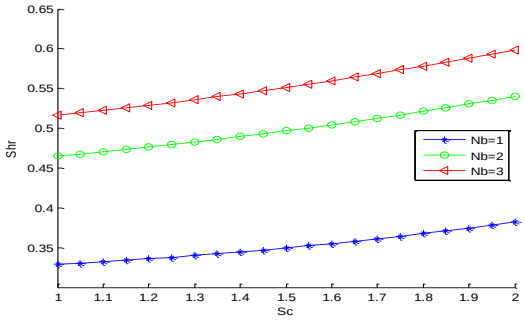

Figure 15. Effect of Brownian motion parameter (N_b) on Sherwood number when Pr=10, N_t =0.1 and M=R=1

The effect of magnetic parameter (M) is illustrated on the skin friction in Figure 13, it is demonstrated that increasing M causes decrease in skin fluid friction which is higher at the upper plate wall whereas increasing values of thermophoretic parameter (N_t) as observed in Figure 14 causes a similar decrease on the Nusselt number i.e. the fluid heat transfer. Also the effect of Sherwood number on flow is observed in Figure 15. It is illustrated that increasing values of Brownian parameter (N_b) causes an increase on mass flow rate of fluid.

CONCLUSION

This present study analyses nanofluid flow through parallel plates arranged horizontally against each other, under the influence of uniform magnetic flux. The nanofluid flow described by nonlinear ordinary differential equations arising from the mechanics of the fluid are analyzed adopting the homotopy perturbation method (HPM). Various thermal-fluidic parameters such as viscosity parameter, Magnetic parameter, Schmidt number are investigated on flow, heat transfer and concentration. Result reveals skin friction and Nusselt number decreases while Sherwood number increases near walls during heat and mass transfer of Nano mix. This study proves useful in the advancement of transport and heat transfer processes in micro mixing, fuel cells, energy conservation, and pharmaceutical processes amongst other applications.

NOMENCLATURE

C	Concentration
c_p	Specific heat capacity of nanofluid
D_B	Diffusion coefficient of diffusing species
k	Thermal conductivity
$M = \frac{\sigma B_0^2 h^2}{\rho \nu}$	Magnetic parameter
$N_b = (\rho c)_p D_B (C_h) / (\rho c)_f \alpha)$	Brownian motion parameter
$N_t = (\rho c)_p D_T (T_H) / [(\rho c)_f \alpha T_c]$	Thermophoretic parameter
p^*	Nanofluid fluid pressure
$\Pr = \frac{\mu}{\rho_f \alpha}$	Prandtl's number
$R = \frac{ah^2}{\nu}$	viscosity variational parameter
$Sc = \frac{\mu}{\rho_f D}$	Schmidt number
T	Temperature
$u = axf'(\eta)$	x component velocity
$v = -ahf(\eta)$	y component velocity
μ	Dynamic viscosity
ρ_f	Base fluid density
$\eta = \frac{y}{h}$	Similarity variable
$\theta(\eta) = \frac{T - T_h}{T_0 - T_h}$	Dimensionless Temperature
$\phi(\eta) = \frac{C - C_h}{C_0 - C_h}$	Dimensionless Concentration

REFERENCES

[1] Abu-Nada, E., Masoud, Z., Hijazi, Z., (2008). Natural convection heat transfer enhancement in horizontal concentric annuli using nanofluids, International Communication Heat Transfer, 35, 657-665.
[2] Cortell, R., (2014). Fluid flow and radiative nonlinear heat transfer over a stretching sheet, Journal of King Saud University, 26, 161-167.
[3] Ellahi, R., Aziz,S., Zeshan, A., (2013) .Non-Newtonian nanofluid flow through porous medium between two coaxial cylinder with heat transfer and variable viscosity, Journal of Porous Media, 16 , 205-216.
[4] Garoosi. F., Bagheri,G., Rashidi,M.M.,(2015). Two phase simulation of natural convection and mixed convection of nanofluid in square cavity, Powder Technology, 275, 239-256.
[5] Garoosi,F., Rohani, B., Rashidi, M.M., (2015). Two phase modeling of mixed convection nanofluids in a square cavity with internal and external heating, Powder Technology, 275, 304-321.
[6] Garoosi, F., Jahanshaloo, L., Rashidi,M.M., Badakhsh, A. Alli, A. (2015). Numerical simulation of natural convection of the nanofluid in heat exchangers using a Buongiorno model, Applied Mathematics and Computation, 254, 183-203.
[7] Malvadi, A., Ganji, D.D., (2014). Brownian motion and thermophoretic effects of slip flow of alumina/water nanofluid inside a circular microchannel in the presence of magnetic field, International Journal of Thermal Science, 84, 196-206.
[8] Mehmood, A., Ali, A., (2008). Analytic solution of three dimensional viscous flow and heat transfer over a stretching surface by homotopy analysis method, American Society of Mechanical Engineers, 130 , 21701-21707.
[9] Rashidi, M.M., Abelman, S., Freidooni, S., Mehr, N., (2013). Entropy generation in steady MHD flow due to rotating porous disk in a nanofluid, International Journal of Heat and Mass Transfer, 62, 515- 525.
[10] Rashidi, S., Dehghan,M., Ellahi, R., Biaz, M., Jamal-Abad, M.T., (2015) .Study of streamwise transverse fluid with convective surface boundary condition, International Journal of Heat and Mass Transfer, 378 ,128-137.
[11] Shehzad, S.A., Alsaedi, A., Hayat, T., (2012). Three dimensional flow of Jeffery fluid with convective surface boundary condition, International Journal of Heat and Mass Transfer, 55, 3971-3976.
[12] Shehzad, S.A., Qasim, M., Alsaedi, A., Hayat, T., Alhuthali, M.S., (2013). Combined effects of thermal stratification and thermal radiation in mixed convection flow of thixotrophic fluid, European Physics Journal, 128-137.
[13] Shehzad, S.A., Alsaedi, F.E., Hayat, T., Monaquel, S.J., (2014). MHD mixed convection flow of thixotrophic fluid with thermal radiation, Heat Transfer Research, 45, 659-676.
[14] Sheikholeslami, M., Ashorynejad, H.R., Domairry, G., Hashim, I., Flow and heat transfer of Cu-water nanofluid between a stretching sheet and a porous surface in rotating system, Journal of Applied Mathematics. Article ID: 421320.
[15] Sheikholeslami, M., Gorji-Bandpy, M., Soleimani, S., (2013). Two phase simulation of nanofluid flow and heat transfer using heat analysis, International Communication of Heat and Mass Transfer, 47, 73-81.
[16] Akbar, N., Rahman, S.U., Ellahi, R., Nadeem, S., (2014). Nanofluid flow in tapering stenosed arteries with permeable walls, International Journal of Thermal Science, 85 ,54-61.
[17] Ashorynojad, H.R., Sheikholeslami, M., Pop, M., Ganji, D.D., (2013). Nanofluid flow and heat transfer due to stretching cylinder in the presence of magnetic field, Heat Mass Transfer Research, 49, 427-436.
[18] Ashorynojad, H.R., Mohamad, A.A., Sheikholeslami, M., (2013). Magnetic field effects on natural convection flow of a nanofluid in a horizontal cylindrical annulus using Lattice Boltzmann method, International Journal of Thermal Science, 64, 240-250.
[19] Domairry, D., Sheikholeslami, M., Ashorynejad, M.R., Suba Reddy Goria, R., (2012). Natural convection of flow of a non-Newtonian nanofluid between two vertical parallel plates, Proceeding of Institute of Mechanical Engineers Part N: Journal of Nanoengineering Nanosystem, 225, 115-122.
[20] Elllahi, R., (2013). The effect of MHD and temperature dependent viscosity on flow of non-Newtonian nanofluid in a pipe: analytical solutions, Applied Mathematical Model, 37, 2013, pp. 1451-1457.
[21] Ellahi, R., Reza, M., Vafai, K., (2012). Series solution of non-Newtonian nanofluids with Reynolds model and Vogel's model by means of homotopy analysis method, Mathematical Computational Model, 55, 1876-1891.
[22] Ellahi, R., Hassan, M., Zeeshan, A., (2015). Shape effect of nanosize particles on Cu-H20 nanofluid on entropy generation, International Journal of Heat and Mass Transfer, 81, 449-456.
[23] Hatami, M., Sheikholeslami, M., Hosseini, M., Ganji, D.D., (2014). Analytical investigation of MHD nanofluid flow in non-parallel walls, Journal of Molecular Liquids, 194, 251-259.
[24] Hatami, M., Shikholeslami, M., Ganji, D.D., (2014). Nanofluid flow and heat transfer in asymmetrical porous channel with expanding or contracting wall, Journal of Molecular Liquid, 195, 230-239.

[25] Hatami, M., Shikholeslami, M., Ganji, D.D., (2014). Laminar flow and heat transfer of nanofluid between contracting and rotating disks by least square method, Powder Technology. 253, 769-779.
[26] Jou, R.Y., Teng, S.C., (2006). Numerical research of natural convective heat transfer enhancement filled with nanofluid in rectangular enclosures, International Communications in Heat and Mass Transfer, 33, 727-736.
[27] Ketayari, G.H.R., (2013). Lattice Boltzmann simulation of natural convection in a nanofluid filled inclined cavity at presence of magnetic field, Science Iran, 20, 1517-1527.
[28] Ketayari, G.H.R., (2013). Lattice Boltzmann simulation of natural convection in nanofluid filled 2D long enclosures at presence of magnetic source. Theoretical Computational Fluid Dynamics, 27, 865-883.
[29] Ketayari, G.H.R., (2013). Lattice Boltzmann simulation of MHD natural convection in nanofluid filled cavity with sinousoidal temperature distribution, Powder Technology, 243, 171-183.
[30] Khan, W.A., Pop, I., (2010). Boundary layer flow of a nanofluid past a stretching sheet. International Journal of Heat Mass Transfer, 53, 2477-2483.
[31] Sheikholeslami, M., Ganji, D.D., (2013). Heat transfer of Cu-water nanofluid flow between parallel plates, Powder Technology, 235, 873-879.
[32] Chand, R., Rana, G., Hussein, A.K. (2015). On the onset of thermal Instability in a low Prandtl number nanofluid layer in a porous medium. Journal of Applied Fluid Mechanics, 8 (2), 265-272.
[33] Mohammed, H., Al-Aswadi, A., Abu-Mulaweh, H., Hussein, A.K., Kanna, P. (2014). Mixed convection over a backward-facing step in a vertical duct using nanofluids-buoyancy opposing case, Journal of Computational and Theoretical Nanoscience, 11, 1-13.
[34] Hussein, A.K., Ashorynejad, H., Shikholeslami, M., Sivasankaran, S. (2014). Lattice Boltzmann simulation of natural convection heat transfer in an open enclosure filled with Cu–water nanofluid in a presence of magnetic field. Nuclear Engineering and Design, 268, 10-17.
[35] Chand, R., Rana, G. a, Hussein, A.K. (2015). Effect of Suspended Particles on the Onset of Thermal Convection in a Nanofluid Layer for More Realistic Boundary Conditions. International Journal of Fluid Mechanics Research, 42 (5),375-390.
[36] Akinshilo, A.T., Olofinkua, J.O., Olaye, O., (2017). Flow and Heat Transfer Analysis of Sodium Alginate Conveying Copper Nanoparticles between Two Parallel Plates. Journal of Applied and Computational Mechanics, DOI:10.22055/jacm.2017.21514.1105.
[37] Sheikholeslami, M., Rashidi, M.M., Alsaad, D.M., Firouzi, F., Rokni, H.B., Domairry, G., (2015). Steady nanofluid flow between parallel plates considering thermophoresis and Brownian effect. Journal of King Saud, http.dx.doi.org/10.1016/j.jksus.2015.06.003.
[38] Hussein, A.K., Bakier, M., Ben Hamida, M., Sivasankaran, S. (2016). Magneto-hydrodynamic natural convection in an inclined T-shaped enclosure for different nanofluids and subjected to a uniform heat source, Alexandria Engineering Journal, 55, 2157-2169.
[39] Hussein, A.K., (2017). Mustafa, A. Natural convection in fully open parallelogrammic cavity filled with Cu-water nanofluid and heated locally from its bottom wall, Thermal Science and Engineering Progress, 1, 66-77.
[40] Kargar, A., Akbarzade, M., (2012). Analytical solution of Natural convection Flow of a non-Newtonian between two vertical parallel plates using the Homotopy Perturbation Method. World Applied Sciences Journal. 20, 1459-1465.
[41] Arslanturk, A., (2005). A decomposition method for fin efficiency of convective straight fin with temperature dependent thermal conductivity. International Communications in Heat and Mass Transfer, 32, 831-841.
[42] Aziz, A., Enamul-Huq, S.M., (1973). Perturbation solution for convecting fin with temperature dependent thermal conductivity. Journal of Heat Transfer, 97, 300-310.
[43] Zhou, J.K., (1986). Differential Transformation and its application for Electrical circuits, Huazhong University Press, China.